Research Article | Vol. 25, No. 17 | 21 Aug 2017 | OPTICS EXPRESS 20791

Optics EXPRESS

Improvement of the temporal and spatial contrast of the nonlinear Fourier-filter

Barnabás Gilicze,[1,*] Rita Dajka,[1] István B. Földes,[2] and Sándor Szatmári[1]

[1]*Department of Experimental Physics, University of Szeged, Dóm tér 9, H-6720 Szeged, Hungary*
[2]*Wigner Research Centre for Physics of the Hungarian Academy of Sciences, H-1525 Budapest P.O.B. 49, Hungary*
**bgilicze@titan.physx.u-szeged.hu*

Abstract: Recently a novel method called nonlinear Fourier-filtering was suggested for temporal and spatial cleaning of high-brightness laser pulses. In this paper experimental demonstration of the associated spatial filtering of this method and significant improvement of the temporal filtering feature are presented. The formerly found limit of ~10^3 for the temporal contrast improvement is identified as diffraction effects caused by the limited numerical aperture of imaging. It is shown by numerical simulation that proper apodization of the object can lead to sufficiently higher limit (>10^8). Using an advanced experimental arrangement the improvement of >2 orders of magnitude is experimentally verified in the ultraviolet and an indirect proof is presented that the background caused by the optical arrangement is reduced below 10^{-7}.

OCIS codes: (070.6110) Spatial filtering; (110.4280) Noise in imaging systems; (140.2180) Excimer lasers; (140.3610) Lasers, ultraviolet; (190.7110) Ultrafast nonlinear optics; (320.5540) Pulse shaping.

References and links

1. V. Yanovsky, V. Chvykov, G. Kalinchenko, P. Rousseau, T. Planchon, T. Matsuoka, A. Maksimchuk, J. Nees, G. Cheriaux, G. Mourou, and K. Krushelnick, "Ultra-high intensity- 300-TW laser at 0.1 Hz repetition rate," Opt. Express **16**(3), 2109–2114 (2008).
2. Z. Wang, C. Liu, Z. Shen, Q. Zhang, H. Teng, and Z. Wei, "High-contrast 1.16 PW Ti:sapphire laser system combined with a doubled chirped-pulse amplification scheme and a femtosecond optical-parametric amplifier," Opt. Lett. **36**(16), 3194–3196 (2011).
3. M. Martinez, W. Bang, G. Dyer, X. Wang, E. Gaul, T. Borger, M. Ringuette, M. Spinks, H. Quevedo, A. Bernstein, M. Donovan, and T. Ditmire, "The Texas petawatt laser and current experiments," AIP Conf. Proc. **1507**, 874–878 (2012).
4. F. Wagner, C. P. João, J. Fils, T. Gottschall, J. Hein, J. Körner, J. Limpert, M. Roth, T. Stöhlker, and V. Bagnoud, "Temporal contrast control at the PHELIX petawatt laser facility by means of tunable sub-picosecond optical parametric amplification," Appl. Phys. B **116**(2), 429–435 (2014).
5. T. M. Jeong and J. Lee, "Femtosecond petawatt laser," Ann. Phys. **526**(3–4), 157–172 (2014).
6. T. Ceccotti, A. Lévy, H. Popescu, F. Réau, P. D'Oliveira, P. Monot, J. P. Geindre, E. Lefebvre, and P. Martin, "Proton Acceleration with High-Intensity Ultrahigh-Contrast Laser Pulses," Phys. Rev. Lett. **99**(18), 185002 (2007).
7. A. Flacco, F. Sylla, M. Veltcheva, M. Carrié, R. Nuter, E. Lefebvre, D. Batani, and V. Malka, "Dependence on pulse duration and foil thickness in high-contrast-laser proton acceleration," Phys. Rev. E Stat. Nonlin. Soft Matter Phys. **81**(3), 036405 (2010).
8. J. S. Green, A. P. L. Robinson, N. Booth, D. C. Carroll, R. J. Dance, R. J. Gray, D. A. MacLellan, P. McKenna, C. D. Murphy, D. Rusby, and L. Wilson, "High efficiency proton beam generation through target thickness control in femtosecond laser-plasma interactions," Appl. Phys. Lett. **104**(21), 214101 (2014).
9. K. B. Wharton, C. D. Boley, A. M. Komashko, A. M. Rubenchik, J. Zweiback, J. Crane, G. Hays, T. E. Cowan, and T. Ditmire, "Effects of nonionizing prepulses in high-intensity laser-solid interactions," Phys. Rev. E Stat. Nonlin. Soft Matter Phys. **64**(2), 025401 (2001).
10. I. B. Földes, J. S. Bakos, K. Gál, Z. Juhász, M. A. Kedves, G. Kocsis, S. Szatmári, and G. Veres, "Properties of high harmonics generated by ultrashort UV laser pulses on solid surfaces," Laser Phys. **10**(1), 264–269 (2000).
11. H. C. Kapteyn, A. Szoke, R. W. Falcone, and M. M. Murnane, "Prepulse energy suppression for high-energy ultrashort pulses using self-induced plasma shuttering," Opt. Lett. **16**(7), 490–492 (1991).
12. C. Thaury, F. Quéré, J.-P. Geindre, A. Levy, T. Ceccotti, P. Monot, M. Bougeard, F. Réau, P. d'Oliveira, P. Audebert, R. Marjoribanks, and P. Martin, "Plasma mirrors for ultrahigh-intensity optics," Nat. Phys. **3**(6), 424–429 (2007).

#293410 https://doi.org/10.1364/OE.25.020791
Journal © 2017 Received 24 Apr 2017; revised 29 Jun 2017; accepted 9 Jul 2017; published 17 Aug 2017

Optics EXPRESS

13. A. Marcinkevičius, R. Tommasini, G. D. Tsakiris, K. J. Witte, E. Gaižauskas, and U. Teubner, "Frequency doubling of multi-terawatt femtosecond pulses," Appl. Phys. B **79**(5), 547–554 (2004).
14. D. Hillier, C. Danson, S. Duffield, D. Egan, S. Elsmere, M. Girling, E. Harvey, N. Hopps, M. Norman, S. Parker, P. Treadwell, D. Winter, and T. Bett, "Ultrahigh contrast from a frequency-doubled chirped-pulse-amplification beamline," Appl. Opt. **52**(18), 4258–4263 (2013).
15. A. Ricci, A. Jullien, J.-P. Rousseau, Y. Liu, A. Houard, P. Ramirez, D. Papadopoulos, A. Pellegrina, P. Georges, F. Druon, N. Forget, and R. Lopez-Martens, "Energy-scalable temporal cleaning device for femtosecond laser pulses based on cross-polarized wave generation," Rev. Sci. Instrum. **84**(4), 043106 (2013).
16. Y. Xu, Y. Leng, X. Guo, X. Zou, Y. Li, X. Lu, C. Wang, Y. Liu, X. Liang, R. Li, and Z. Xu, "Pulse temporal quality improvement in a petawatt Ti: Sapphire laser based on cross-polarized wave generation," Opt. Commun. **313**, 175–179 (2014).
17. M. P. Kalashnikov, E. Risse, H. Schönnagel, and W. Sandner, "Double chirped-pulse-amplification laser: a way to clean pulses temporally," Opt. Lett. **30**(8), 923–925 (2005).
18. Y. Chu, X. Liang, L. Yu, Y. Xu, L. Xu, L. Ma, X. Lu, Y. Liu, Y. Leng, R. Li, and Z. Xu, "High-contrast 2.0 Petawatt Ti:sapphire laser system," Opt. Express **21**(24), 29231–29239 (2013).
19. S. Szatmári, R. Dajka, A. Barna, B. Gilicze, and I. B. Földes, "Improvement of the temporal and spatial contrast for high-brightness laser beams," Laser Phys. Lett. **13**(7), 075301 (2016).
20. S. Szatmári and F. P. Schäfer, "Simplified laser system for the generation of 60 fs pulses at 248 nm," Opt. Commun. **68**(3), 196–202 (1988).
21. S. V. Alekseev, A. I. Aristov, Ya. V. Grudtsyn, N. G. Ivanov, B. M. Koval'chuk, V. F. Losev, S. B. Mamaev, G. A. Mesyats, L. D. Mikheev, Yu. N. Panchenko, A. V. Polivin, S. G. Stepanov, N. A. Ratakhin, V. I. Yalovoi, and A. G. Yastremskii, "Visible-range hybrid femtosecond systems based on a XeF(C–A) amplifier: state of the art and prospects," Quantum Electron. **43**(3), 190–200 (2013).
22. J. Békési, S. Szatmári, P. Simon, and G. Marowsky, "Table-top KrF amplifier delivering 270 fs output pulses with over 9 W average power at 300 Hz," Appl. Phys. B **75**(4), 521–524 (2002).
23. S. Szatmári, Z. Bakonyi, and P. Simon, "Active spatial filtering of laser beams," Opt. Commun. **134**(1–6), 199–204 (1997).
24. S. Szatmár, G. Almási, M. Feuerhake, and P. Simon, "Production of intensities of 10^19 W/cm^2 by a table-top KrF laser," Appl. Phys. B **63**(5), 463–466 (1996).
25. I. B. Földes, D. Csáti, F. L. Szűcs, and S. Szatmári, "Plasma mirror effect with a short-pulse KrF laser," Rad. Effects & Defects in Solids **165**(6–10), 429–433 (2010).
26. B. Gilicze, A. Barna, Z. Kovács, S. Szatmári, and I. B. Földes, "Plasma mirrors for short pulse KrF lasers," Rev. Sci. Instrum. **87**(8), 083101 (2016).
27. J. W. Goodman, *Introduction to Fourier Optics* (Roberts and Company, 2005), Chap. 6.

1. Introduction

The remarkable progress of high-intensity laser systems allowed the investigation of laser-plasma interaction up to the relativistic regime [1–5]. Experiments show that temporal contrast improvement is the key to accessing higher intensity during such interactions [6–8]. The achieved and the planned intensities are already in the 10^{22}-10^{25} W/cm^2 range. Pre-pulses and ASE of 10^7-10^8 W/cm^2 intensities can change laser-matter interactions considerably [9,10], which sets the necessary temporal contrast beyond 10^{14}. Several techniques have been proposed to improve the contrast of CPA based laser systems. The plasma mirror [11,12] and harmonic frequency generation [13,14] are usually used after the final compressor. Cross-polarized wave generation (XPW) is used between two CPA stages (Double-CPA, DCPA) to inject relatively high-energy, high-contrast pulses to the second amplifier stage [15,16]. DCPA systems have 10^{10}-10^{12} temporal contrast on a ns-scale, but the coherent pedestal in the ps vicinity of the main pulse still remains [16–18]. For more detailed comparison of the former contrast improvement techniques such as saturable absorber, nonlinear Sagnac interferometer and nonlinear ellipse rotation, see [19] and the references therein.

In short-pulse excimer laser systems the generation and the final amplification of the pulse is performed at two different wavelengths, necessitating intermediate frequency doubling [20,21] or tripling [22]. Using a novel method for frequency conversion – referred to as active spatial filtering [23] - effective temporal and spatial filtering occurs before UV amplification. In these systems the CPA scheme is not required, since the low saturation energy density of excimers allows direct amplification of femtosecond pulses. For these reasons output pulses of excellent spatial and temporal quality are available for medium output power, allowing to reach >10^{19} W/cm^2 focused intensity and >10^{10} temporal contrast for several times 10 mJ output energy at 248 nm [24]. On the other hand, in case of additional amplification the

Optics EXPRESS

rapidly growing ASE in the UV amplifiers sets the temporal contrast below 10^{10}. Plasma mirror technique was also successfully applied for short-pulse excimer lasers [25] demonstrating ~70% reflectivity and 10^2-10^3 temporal contrast improvement [26].

A novel technique called nonlinear Fourier-filtering has been recently presented [19], and successfully applied in the UV. This technique is demonstrated to provide simultaneous effective temporal and spatial filtering and seems to be energy and wavelength scalable. In this arrangement selective nonlinear phase-shift in the Fourier plane is introduced by the self-generated plasma in a pulsed gas jet as shown in Fig. 1. An annular beam (formed by an input beam block or preferably with axicon lenses) is focused into the gas jet where the nonlinear modulation of the phase of the different diffraction orders leads to directional modulation of the beam. The low intensity ASE is not (or negligibly) modulated, therefore the same annular beam is imaged at the output. It is only diffraction which determines the output distribution for the low intensity part of the beam. If the inverse of the input beam-block - practically an iris diaphragm - is applied at the output, it ensures efficient exclusion of the ASE. However, if the main pulse which undergoes - in an ideal case π - phase shift by the self-generated plasma, a significantly modified output distribution occurs, and as high as >40% of the energy is transmitted through the output diaphragm. In [19] this phenomenon was theoretically treated by connecting the output beam to the input one by a subsequent use of a 2D FFT, an intensity dependent phase shift and a 2D IFFT. The temporal contrast improvement (given by the ratio of the high and the low intensity transmission of the system) was found to be limited by the low intensity transmission; primary by the unwanted diffraction effects associated with imaging. The achievable temporal contrast improvement was estimated to 10^3 for the "standard imaging" case.

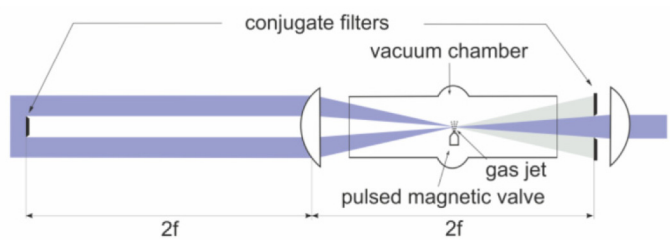

Fig. 1. Schematic of the nonlinear Fourier-filter (taken from ref [19].)

This paper is a report on the improvement of the spatial and temporal filtering features of the nonlinear Fourier-filter. The excellent spatial quality of the filtered beam is confirmed by measuring its far field distribution. We found that proper modulation of the spatial frequency components of the input beam block (apodization) significantly improves the theoretical limit for the temporal contrast improvement. Using an advanced experimental arrangement - where the apodized object is created by proper pre-imaging - a lower limit of 10^5 is verified for temporal contrast improvement which is determined by the limited dynamic range of the measurement. An indirect proof is presented that as low as 10^{-7} level of background associated with imaging can be reached.

2. Theoretical study

In principle the achievable temporal contrast improvement for a temporal filtering technique is limited by the order of nonlinearity of the applied process. However this upper limit is not or barely reached for practical cases. The limited extinction ratio of polarizers in case of XPW or the low intensity reflection of plasma mirrors sets the temporal contrast improvement to ~10^4 and ~10^2 (for a single stage) respectively. The temporal contrast improvement for the nonlinear Fourier-filter was previously found to be 10^3. The origin of the background was

Optics EXPRESS

identified as diffraction effects during imaging. The spatial frequency analysis of imaging systems [27] provides a convenient way to understand and to estimate this phenomenon.

In general an imaging system can be described by a transfer function of finite bandwidth, therefore the system has limited capabilities to transfer the high spatial frequency components of an object. The transfer function is substantially different for spatially coherent (Amplitude Transfer Function, ATF) and for spatially incoherent (Optical Transfer Function, OTF) illumination. In case of spatially coherent illumination the transfer function is constant up to the $f_0 = 1/(2\lambda F)$ cut-off frequency, where it drops to zero (λ is the wavelength and F is the F-number of the system). In case of spatially incoherent illumination the cut-off frequency is $2f_0$ but the function is monotonically decreasing until it reaches the cut-off. Figure 2 shows the calculated spatial intensity distribution of the image of an annular beam with step-like edges in case of coherent and incoherent illumination for two image systems of different cut-off frequency. The numerical calculation was based on 2D Fast Fourier Transformation (FFT). The inverse Fourier transform of the image can be calculated by the product of the Fourier transform of the object and the transfer function of the image system. The $f_0 = 500\,\mathrm{cm}^{-1}$ cut-off frequency represents our experimental case. It is seen from the blue curves of Fig. 1 that objects containing high spatial frequencies (sharp edges) can be imaged by a radiation of medium frequency only with poor spatial contrast. This can be improved by increasing the cut-off frequency of the image system (see red curves). The coherent illumination always results in better spatial contrast.

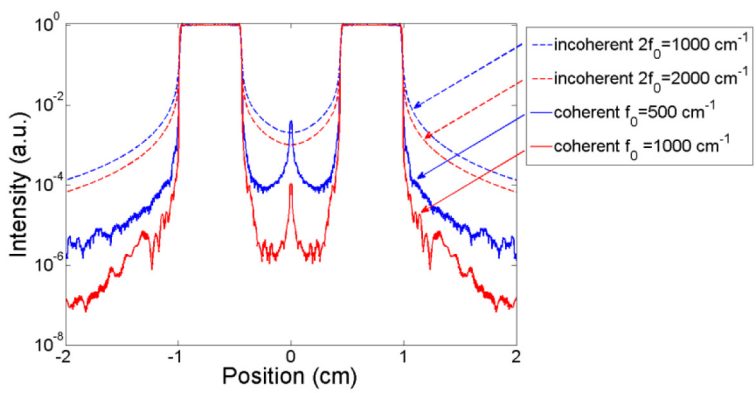

Fig. 2. Calculated spatial intensity distribution of the image of an annular beam in case of coherent (solid lines) and incoherent (dashed lines) illumination for an image system of $f_0 = 500\,\mathrm{cm}^{-1}$ (blue) and of $f_0 = 1000\,\mathrm{cm}^{-1}$ (red) cut-off frequencies.

Apodization can be of great importance to reach much better spatial contrast for an image system. Apodization refers to the introduction of controlled attenuation of the edges of the exit pupil for a given image system. However, the realization of apodization of the exit pupil (the aperture of the imaging lens in this case) is technically difficult. Our suggestion is to reduce the highest spatial frequency components of the object. The simplest solution would be to change the sharp input beam-block in Fig. 1 to an apodized one whose spatially dependent transmission follows the green curve instead of the blue one of Fig. 3(a). Another possible and more preferable realization is to introduce an imaging of low numerical aperture (NA) prior to Fourier-filtering (called pre-imaging) to exclude the higher spatial frequencies of the intermediate picture created by this pre-image system. This image completed by a second annular beam-block serves as an apodized object for the nonlinear Fourier-filter. The secondary beam-block provides full exclusion of the background of 10^{-3} level in the center.

Optics EXPRESS

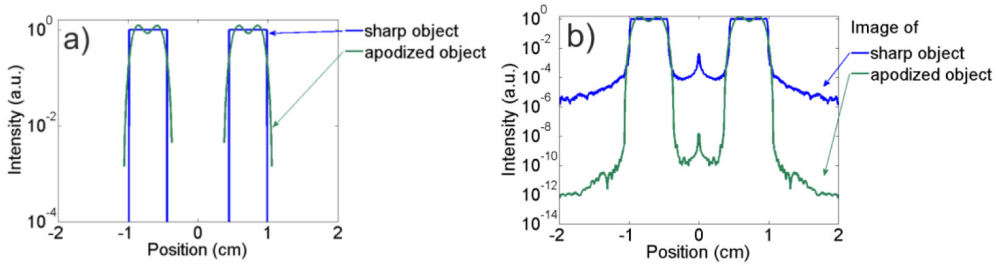

Fig. 3. Calculated intensity distribution of an apodized object created by the pre-imaging and by the secondary beam-block (a) and of the corresponding image created by the nonlinear Fourier-filter for the coherent case (b) (green curves). A sharp object (a) and its image (b) are shown for comparison (blue curves).

Figure 3(a) shows the calculated intensity distribution of such apodized object created by the pre-imaging and the secondary beam-block. The low NA pre-imaging is modeled by allowing transmission only the first 10 diffraction maxima in the Fourier-plane of the lens. (The spatial distribution in this plane is the Fourier-transform of that in the lens plane). Figure 3(b) shows the corresponding calculated intensity distribution of the image created by the focusing lens of the nonlinear Fourier-filter for the coherent case ($f_0 = 500\,\mathrm{cm}^{-1}$). The calculation shows remarkable improvement; the spatial contrast of imaging is increased by ~5 orders of magnitude to the $>10^8$ level. In case of incoherent illumination the reduction of the highest spatial frequency components is not as effective (1 order of magnitude improvement). This, however, is not a serious practical problem, since the background is coherent on the ps scale for CPA based systems and the ASE can be made highly coherent by the pre-imaging procedure.

3. Experimental results and discussion

The spatial filtering feature (beam smoothing) of the nonlinear Fourier-filter was experimentally characterized. Figures 4(a) and 4(b) show the focal distribution of the input annular beam and of the output beam (passing through the center of the output diaphragm). In this measurement focusing was done with an f/35 optics. The output distribution is found to be nearly Gaussian Both the input and the output beams were found to be ~1.75 times diffraction limited. The spectral intensity distribution was also measured before and after the filtering and no detectable change was found. These features offer good focusability and the possibility of further amplification of the beam.

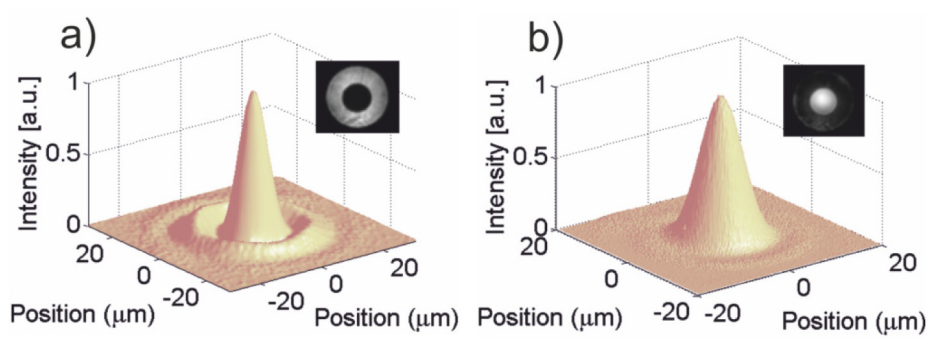

Fig. 4. Focal distribution of the input annular beam (a) and of the output beam (passing through the center of the output diaphragm) (b) (insets in the right upper corner are the corresponding near-field distributions).

Optics EXPRESS

Direct measurement of temporal contrast above 10^{12} even in the IR is highly challenging. Considering that direct measurement of the temporal contrast of similar dynamic range in the UV is not available at the time of this publication and the initial temporal contrast of our KrF femtosecond laser system is above 10^{10}, direct measurement of the contrast of the temporally improved pulse is not possible. However, one advantage of KrF femtosecond laser systems is that the only source of the temporal background is the ASE. This makes easy to determine the intensity of the temporal noise by utilizing the known/measured smooth intensity distribution within the temporal window and solid angle of ASE. (In case of our laser system the initial ratio of the energy, pulse length and solid angle for the ASE to main pulse are 1mJ/10mJ, 15ns/500fs and $5\cdot10^4$, respectively.) Therefore the contrast improvement of the nonlinear Fourier-filter was determined by measuring its intensity dependent transmission. Figure 5 shows the transmission of the nonlinear Fourier-filter as a function of intensity (black squares). The transmission is defined as the ratio of the output and input energy measured by photodiodes simultaneously. After the temporal filtering (shown in Fig. 1) the beam was focused through a pinhole and a Hamamatsu R1193U-52 type photodiode was positioned after the pinhole of proper size. This pinhole served as a spatial filter to measure only that background which propagates in the same direction as the main pulse. It can be seen from Fig. 5 that the transmission decreases with a slope connected to the nonlinearity of the process. However, a constant background of different origin stops further decrease of the transmission, which is found to be present even if the gas jet is not operated. This background limits the temporal contrast improvement to ~10^3 for "ordinary" imaging.

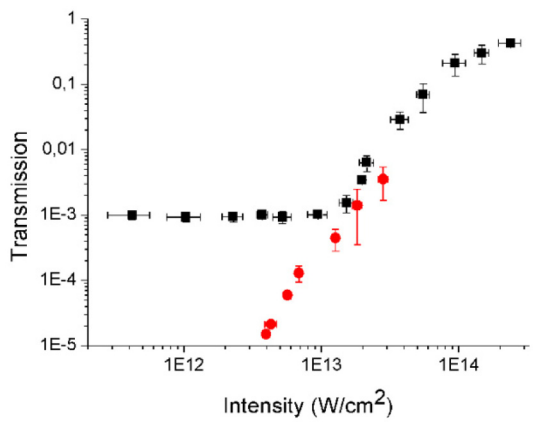

Fig. 5. Measured transmission of the nonlinear Fourier-filter versus intensity without (black squares) and with apodization (red dots).

Figure 6 shows the experimental realization of the nonlinear Fourier-filter completed by the low NA pre-imaging. Note that this pre-imaging of limited NA has threefold advantage over other approaches; beyond the main task that an "unsharp" picture of reduced spatial frequency components has created (which can later be imaged with better spatial contrast) this pre-imaging also makes the unwanted noise spatially coherent - promoting high contrast imaging - moreover, it acts as a standard spatial filter reducing ASE coupling between the amplifiers. The low NA pre-imaging arrangement has a practical advantage that it is found to be relatively insensitive for eventual misalignments; our calculation showed practically no change in the contrast for a misaligned aperture limiting pinhole. Figure 5 (red dots) shows the intensity dependent transmission of this advanced nonlinear Fourier-filter corresponding to Fig. 6. Due the energy loss caused by the UV optics of pre-imaging and to the limited dynamic range of photodiodes the transmission measurement is realized only in the range from 10^{-2} to 10^{-5}. This measurement gives a lower limit of 10^{-5} for the transmission background. In order to maintain the high intensity transmission (~40%) of this advanced

Optics EXPRESS

system the energy loss of UV optics is crucial to be reduced and/or the input energy has to be increased by an additional amplification stage before the filtering.

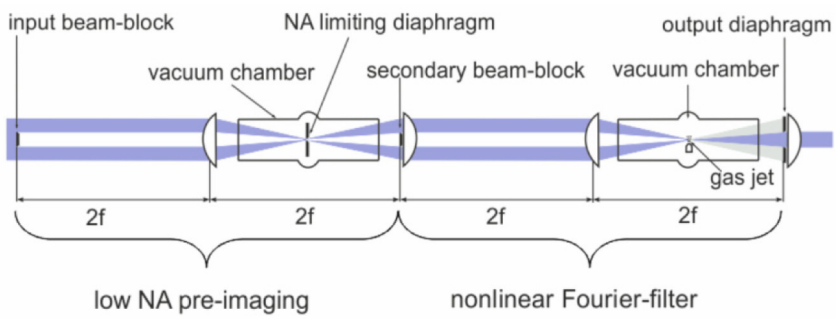

Fig. 6. Experimental realization of the Nonlinear Fourier-filter completed by pre-imaging of low NA.

Note that the measured 10^{-5} level background of the imaging is determined by the dynamic range of the measurement. The slope of the transmission curve does not seem to decrease. The experimentally achievable spatial contrast by such an image system was further studied using an amplitude modulated diode laser (λ = 650 nm). The modulated light was detected by a BPW21R photodiode whose signal was amplified in a narrowband amplifier, where the polarity of the amplified signal was alternately switched and sent to the input of an integrator in synchron of the modulation of the light source. This frequency- and phase-sensitive detection technique allowed us to exclude the background of any other light sources different than the diode laser and to extend the dynamical range of our measurement. With this arrangement the background in the image plane was found to be still lower than the detection limit, giving an indirect proof of $>10^7$ temporal contrast improvement.

4. Conclusion

In conclusion the focusability measurements showed excellent spatial distribution for the filtered beam. The limitations for temporal filtering of the nonlinear Fourier-filter were investigated both theoretically and experimentally by the spatial frequency analysis of image systems. Temporal contrast improvement up to 10^5 was demonstrated. The possibility to reach $>10^7$ temporal contrast improvement was presented by an indirect measurement. These features together with the relatively high (>40%) internal energy efficiency make possible the application of this filtering technique in a wide wavelength range both before and after the final amplification.

Funding

Hungarian Scientific Research Fund (OTKA113222) and by the European Union's Horizon 2020 research and innovation programme under grant agreement no 654148 Laserlab-Europe. This work was carried out within the framework of the EUROfusion Consortium and has received funding from the Euratom research and training programme 2014-2018 under grant agreement 633053.

Acknowledgments

The authors would like to thank Zsolt Homik for his contribution to the transmission measurements.